On optimal sensor placement and motion coordination for target tracking

Sulema Aranda Sonia Martínez Francesco Bullo
Mechanical and Environmental Engineering
University of California at Santa Barbara
Santa Barbara, CA, 93106-5070, USA
{smartine,bullo}@engineering.ucsb.edu

Technical Report CCEC-04-1013, Original version, October 13, 2004
Revised version, August 14, 2007 (Corrected statement of Proposition 2.3)

***Abstract*—This work studies optimal sensor placement and motion coordination strategies for mobile sensor networks. For a target tracking application with range sensors, we investigate the determinant of the Cramer-Rao Lower Bound and compute it in the 2D and 3D cases. We characterize the global minima of the 2D case. We propose and characterize motion coordination algorithms that steer the mobile sensor network to an optimal deployment and that are amenable to a decentralized implementation. Finally, our numerical simulations illustrate how the proposed motion coordination algorithms lead to the improved performance of an extended Kalman filter in a target tracking scenario.**

motion coordination, optimal sensor placement, Cramer-Rao Lower Bound, Kalman filtering.

I. Introduction

New advancements in the fields of microelectronics and miniaturization have generated a tremendous surge of activity in the design and development of sensor networks. The envisioned groups of agents are endowed with communication, sensing and computation capabilities, and promise great efficiency in the realization of multiple tasks such as environmental monitoring, exploratory missions and search and rescue operations. However, several fundamental problems need to be solved in order to make this future technology possible.

One main difficulty is the requirement for decentralized architectures in which each agent takes autonomous decisions based on information shared with only a few local neighbors. Ongoing research work focuses on decentralized filters and data-fusing methods for estimation, and on the motion algorithms that guarantee the desired global behavior of the network. Ideally, both the motion control algorithms and estimation processes should be optimally integrated to make the most of the network performance.

In this paper we investigate the design of distributed motion coordination algorithms that increase the information gathered by a network in static and dynamic target-tracking scenarios. In order to do this, we define an aggregate cost function that encodes a "sensitivity performance measure" and design motion coordination algorithms maximizing it.

This idea has been widely used in papers on optimum experimental design for dynamical systems with applications to measurement problems. An incomplete list of references is [1], [2], [3], [4], [5], [6]. For example [3], [4], [5] deal with problems on target tracking and parameter identification of distributed parameter systems. The motion control algorithms proposed in these papers either are computed via some off-line numerical method or are gradient algorithms. Often these algorithms are designed to maximize an appropriate scalar cost function and to choose the best sensor locations from a grid of finite candidates. Unfortunately, these schemes turn out to be not distributed since in order to define the control law for each agent, it is necessary to know all other agents' positions at each step.

A second set of relevant references are those on distributed motion coordination. To define our proposed control algorithm we build on recent results on the analysis of cyclic pursuit [7], flocking [8], and consensus [9].

The contributions of this paper are the following. Under the assumption of Gaussian noise measurements with diagonal correlation, we obtain in Section II closed-form expressions for the determinant of the Fisher Information Matrix for "range-measurement" models in non-random static scenarios, for 2 and 3 dimensional state spaces. We characterize the critical points of these functions and obtain sets of positions that globally maximize the value of the 2D version. If the sensors measure distances to the target, then a optimal configuration is one in which the sensors are uniformly placed in circular fashion the target.

This optimal configuration serves as a starting point in Section III. Here we consider a target tracking scenario described by the following assumptions: the sensors move along the boundary of a convex set containing the target. We define discrete-time control laws that, relying only on local information, achieve the uniform configuration around the target (estimate) exponentially fast. In essence, our laws are very intuitive and simple-to-implement interaction behaviors between the sensors.

Finally, in Section IV, we validate our control laws in a particular dynamic target-tracking scenario. Although we

studied the global optimum configurations for a *nonrandom static* parameter estimation scenario we adopt the results in a *dynamic random* scenario. Our simulations illustrate the following reasonable conjecture: optimizing the sensitivity function for the static non-random case improves the performance of a filter (in our case an EKF) for the dynamic random scenario.

As a final remark, we point out that we do not deal here with the problem of decentralized filters and data-fusion, taking into account communication constraints. It is assumed that the process of estimation is performed by a central site or by a distributed process that we do not implement. For works that deal with multisensor fusion possibly under communication constraints we refer to [10], [11], [12], [13] and references therein.

II. Optimal placement of sensors

Here we present the assumptions over our sensor network and target models in (1) non-random static parameter estimation scenarios and (2) random dynamic parameter estimation scenarios. We obtain the corresponding Fisher Information Matrices (FIMs) and Cramer-Rao Lower Bounds (CRLBs). We analyze the global minima of the determinant of the CRLB as a means to guarantee increased sensitivity with respect to the sensors' measurements. See [14] for a comprehensive treatment on estimation and tracking.

A. The non-random parameter estimation scenario

The localization of static targets can be solved as a non-random parameter estimation problem as follows. Let $p_j \in \mathbb{R}^d$, $j \in \{1,\dots,n\}$, denote the position of n sensors moving in a convex region $Q \subseteq \mathbb{R}^d$ and let $q_0 \in Q$ be the unknown target position to be estimated by means of the measurement model:

$$z_j(q) = h(\|q - p_j\|) + w_j\,, \quad q \in Q\,, \tag{1}$$

for $j \in \{1,\dots,n\}$. Here, $h : [0,+\infty) = \mathbb{R}_+ \to \mathbb{R}$ is defined according to the particular sensors' specifications and w_j represents a white noise, $j \in \{1,\dots,n\}$.

In other words, the stacked vector of measurements at a certain instant is a random vector normally distributed as

$$Z \equiv \begin{bmatrix} z_1 \\ \vdots \\ z_n \end{bmatrix} \sim \mathcal{N}\left(\begin{bmatrix} h(\|q-p_1\|) \\ \vdots \\ h(\|q-p_n\|) \end{bmatrix}, R \right),$$

where $R = R^T > 0$ is the $n \times n$ covariance matrix. From now on, we will use the shorthand notation $Z = (z_1,\dots,z_n)^T$, and H will denote the function $H(q,p_1,\dots,p_n) = (h(\|q-p_1\|),\dots,h(\|q-p_n\|))^T$.

The *Fisher Information Matrix* (FIM) for non-random parameters, denoted by J_{NR}, is defined as the expected value with respect to the probability distribution $p(Z|q)$:

$$J_{\text{NR}} \triangleq E\left[(\nabla_q \log\Lambda)\cdot(\nabla_q \log\Lambda)^T\right]_{q=q_0}\,,$$

where q_0 is the true value of the target location or an estimate of it, $\nabla_q = [\frac{\partial}{\partial q^1},\dots,\frac{\partial}{\partial q^d}]^T$, and Λ is a shorthand for $\Lambda(q,p_1,\dots,p_n) = p(z_1,\dots,z_n|q)$, the *likelihood function*,

$$\Lambda(q,p_1,\dots,p_n) = \frac{1}{\sqrt{2\pi\det P}}\ \exp\left(-\frac{1}{2}(Z-H)^T R^{-1}(Z-H)\right).$$

A few computations show $J_{\text{NR}} = (\nabla_q H)^T_{q_0} R^{-1} (\nabla_q H)_{q_0}$. The matrix $G = (\nabla_q H)_{q_0}$ is usually called the *Sensitivity Matrix* associated with our set of measurements.

Let $q = (q^1,\dots,q^d)^T$, and define the shorthands

$$\partial_\ell h_j(q_0,p_1,\dots,p_n) \triangleq \frac{\partial}{\partial q^\ell} h(\|q-p_j\|)\Big|_{q=q_0},$$

for $j \in \{1,\dots,n\}$ and $\ell \in \{1,\dots,d\}$. Then $G : \mathbb{R}^d \times (\mathbb{R}^n)^d \to \mathbb{R}^{n\times n}$ can be computed to be

$$G_{j\ell}(q_0,p_1,\dots,p_n) = \partial_\ell h_j(q_0,p_1,\dots,p_n)\,,$$

for $j \in \{1,\dots,n\}$ and $\ell \in \{1,\dots,d\}$. In the particular case that $R = \sigma^2 I_n$, the FIM J_{NR} can be expressed as:

$$\begin{aligned} J_{\text{NR}}(q_0,p_1,\dots,p_n) &= \frac{1}{\sigma^2} G^T G(q_0,p_1,\dots,p_n) \\ &= \frac{1}{\sigma^2}\sum_{j=1}^{n} \begin{bmatrix} (\partial_1 h_j)^2 & \dots & (\partial_1 h_j)(\partial_d h_j) \\ \vdots & \ddots & \vdots \\ (\partial_d h_j)(\partial_1 h_j) & \dots & (\partial_d h_j)^2 \end{bmatrix}. \end{aligned} \tag{2}$$

B. The dynamic random parameter estimation scenario

Dynamic targets can be thought of random parameters evolving under a stochastic difference equation. Here we assume that the target position $q(k)$ at time $k \in \mathbb{N}\cup\{0\}$ satisfies:

$$q(k) = F_k(q(k-1)) + v(k)\,, \quad k \geq 1,\ q(0) = q_0\,,$$

for some functions $F_k : \mathbb{R}^d \to \mathbb{R}^d$ and $v(k)$ i.i.d as $v(k) \sim \mathcal{N}(0,N(k))$, where $N(k) = N(k)^T > 0$, $\forall k \geq 0$, and $E[v(k_1)v(k_2)^T] = \delta_{12}N(k_1)$, $\forall k_1,\ k_2 \geq 0$. Similarly as before, we model our sensor network as

$$Z(k) = H_k(q(k),p_1(k),\dots,p_n(k)) + w(k), \quad k \geq 0,$$

with $H_k(q(k),p_1(k),\dots,p_n(k))=(h_k(\|q(k)-p_1(k)\|,\dots,h_k(\|q(k)-p_n(k)\|))$, for some functions $h_k : \mathbb{R}_+ \to \mathbb{R}$, and $Z(k)=(z_1(k),\dots,z_n(k))$, $k \geq 0$. We will assume that $w(k) \sim \mathcal{N}(0,R(k))$, where $R(k) = R(k)^T > 0$, $k \geq 0$, and that $E[w(k_1)w(k_2)^T] = \delta_{12}R(k_1)$, $\forall k_1,\ k_2 \geq 0$.

An estimation method that is widely employed for the detection of targets is that of the Extended Kalman Filter (EKF) [14]. The assumptions for the filter require $q(k)$ and $Z(k)$ to be jointly Gaussian distributed with covariance $P(k) = P(k)^T$, and $E[q(k_1)w(k_2)] = 0$, $\forall k_1,k_2 \geq 0$. The EKF provides a state estimate $\hat{q}(k)$ together with an estimate for the covariance of the error $P_e(k)$:

$$P_e(k) = P_p(k) - W(k)S(k)W(k)^T\,, \quad k \geq 1\,.$$

Here, $P_p(k)$ is the predicted covariance of the error, $W(k) = P_p(k)(\nabla_{q(k)}F_k)^T S^{-1}(k)$ and $S(k) = (\nabla_{q(k)}F_k)P_p(k)(\nabla_{q(k)}F_k)^T + R(k)$. Let $q_p(k)$ be the

predicted value of $q(k)$. Some standard computations [14], [11], allow us to say that

$$P_e^{-1}(k) = P_p^{-1}(k) + (\nabla_q H_{k|q_p(k)})^T R^{-1}(k) \nabla_q H_{k|q_p(k)}$$

or, denoting $(\nabla_q H_{k|q_p(k)})^T R^{-1}(k) \nabla_q H_{k|q_p(k)} = J_{\text{NR}}(k)$,

$$P_e^{-1}(k) = P_p^{-1}(k) + J_{\text{NR}}(k)\,, \quad k \geq 0\,. \tag{3}$$

That is, the FIM for the non-random case appears as a summand in the expression for the inverse of the predicted covariance matrix of the EKF. Similarly, when the measurement model is linear, an analogous set of computations allows us to derive a relationship between the FIM for dynamic random parameters, denoted by J_{DR} at step $k \geq 0$, and $J_{\text{NR}}(k)$ given by

$$J_{DR}(k) = P_{qq}^{-1} + J_{NR}(k)\,, \tag{4}$$

where $P_{qq} = E[(q(k) - \bar{q}_k)(q(k) - \bar{q}_k)^T]$.

C. Cost functions for optimal sensing

As is well known, the FIM encodes the amount of information that a set of measurements produces in estimating a set of parameters. Under the assumptions we have made in former sections FIM = CRLB^{-1}; i.e., the FIM is the inverse of the Cramer Rao Lower Bound, which is known to lower bound the inverse of the covariance of the error[1]

$$J^{-1} = \text{CRLB} \leq E[(\hat{q} - q_0)(\hat{q} - q_0)^T].$$

Because of this, one expects that "minimizing the CRLB" results in a decrease of uncertainty.

This line of reasoning has been a main theme in several papers dealing with *optimum experimental design* and *active sensing* e.g., see [3], [4], [15], [1]. Starting from the FIM (resp. the CRLB) of the estimation approach, an *evaluation function* is defined (usually the determinant or the trace of the FIM/CRLB) whose maximization (resp. its minimization) is to be achieved.[2]

As before, let $q_0 \in \mathbb{R}^d$ be the true value of the target location or an estimate of it. Under the assumptions of Subsection II-A and II-B, we define our cost function $\mathcal{L}_{q_0} : (\mathbb{R}^d)^n \to \mathbb{R}_+$ by

$$\mathcal{L}_{q_0}(p_1, \ldots, p_n) = \det J_{\text{NR}}(q_0, p_1, \ldots, p_n), \tag{5}$$

with J_{NR} given in (2). Because of the relationships (3) and (4), we are guaranteed that, if we optimize $\mathcal{L}_{q_0}$ with respect to the positions of the sensors, then we will get increased performance in both the non-random and dynamic random parameter estimation scenarios with EKFs.

In what follows we derive the expression for the cost function $\mathcal{L}_{q_0}$ for $d = 2$ and $d = 3$ and analyze its critical points and global maxima. To do this, we shall assume that our measurement model is

$$h(r) = \begin{cases} \gamma(r - c_1)^\beta + c_2, & R_0 < r < R_1 \\ 0, & \text{otherwise} \end{cases} \tag{6}$$

[1]For efficient estimators, this inequality becomes an equality.

[2]For $\det J$, this technique is known as the D-optimum design [15].

for $\gamma \in \{-1, +1\}$, $\beta \in \mathbb{Z}$, and constants $R_1 > R_0 > 0$, $c_2, c_1 \in \mathbb{R}_+$. Range sensors such as sonars can be modeled by $\beta = 1$, $\gamma = 1$ and $c_1 = c_2 = 0$.

Proposition 2.1: For $q_0 \in \mathbb{R}^d$, let $\mathcal{L}_{q_0} : (\mathbb{R}^d)^n \to \mathbb{R}_+$ be defined as in (5) and h be defined as in equation (6). Consider the set $\mathcal{S} = \{p_i \in \{p_1, \ldots, p_n\} \,|\, h(\|p_i - q_0\|) \neq 0\}$. The following statements hold true.

(i) For $d = 2$,

$$\mathcal{L}_{q_0}(p_1, \ldots, p_n) = \frac{1}{2\sigma^2} \sum_{i,j \in \mathcal{S}} \|\mathbf{v}_i\|^2 \|\mathbf{v}_j\|^2 \sin^2 \alpha_{ij}$$

where $\alpha_{ij} \triangleq \measuredangle(\mathbf{v}_i, \mathbf{v}_j)$, and $\mathbf{v}_i = (\partial_1 h_i, \partial_2 h_i, 0)$, $\|\mathbf{v}_i\|^2 = \beta^2(\|p_i - q_0\| - c_1)^{2(\beta-1)}$, $i, j \in \mathcal{S}$.

(ii) For $d = 3$,

$$\mathcal{L}_{q_0}(p_1, \ldots, p_n) = \frac{1}{6\sigma^2} \sum_{i,j,k \in \mathcal{S}} \|\mathbf{v}_i\|^2 \|\mathbf{v}_j\|^2 \|\mathbf{v}_k\|^2 \sin^2 \alpha_{ij} \cos^2 \beta_{ij,k}$$

where $\alpha_{ij} \triangleq \measuredangle(\mathbf{v}_i, \mathbf{v}_j)$, $\beta_{ij,k} \triangleq \measuredangle(\mathbf{v}_i \times \mathbf{v}_j, \mathbf{v}_k)$, and $\mathbf{v}_i = (\partial_1 h_i, \partial_2 h_i, \partial_3 h_i)$, with $\|\mathbf{v}_i\|^2 = \beta^2(\|p_i - q_0\| - c_1)^{2(\beta-1)}$, for $i, j, k \in \mathcal{S}$.

The proof can be found in Appendix A.

Let us now introduce some useful notation. Let $\mathbb{T}$ be the circle in the plane and let $\mathcal{L}_{\mathbb{T}} : \mathbb{T}^n \to \mathbb{R}_+$ be defined by

$$\mathcal{L}_{\mathbb{T}}(\delta_1, \ldots, \delta_n) = \frac{\beta^4 R^2}{2\sigma^2} \sum_{i,j \in \mathcal{S}} \sin^2(\delta_i - \delta_j),$$

where $R = \max_{r \in [R_0, R_1]} (r - c_1)^{2(\beta-1)} \geq 0$. Now, let $d = 2$ and assume $q_0 \neq p_i$, for $i \in \{1, \ldots, n\}$. Consider a polar change of coordinates centered at $q_0 \in \mathbb{R}^2$, and identify $p_i \in \mathbb{R}^2$ with (η_i, r_i) for some angle $\eta_i \in \mathbb{T}$ and $r_i \in \mathbb{R}_+$, $i \in \{1, \ldots, n\}$. With these notations, we have that $\mathcal{L}_{q_0}(p_1, \ldots, p_n) \leq \mathcal{L}_{\mathbb{T}}(\eta_1, \ldots, \eta_n)$ and $(p_1, \ldots, p_n)$ is a global maximum of $\mathcal{L}_{q_0}$ if and only if $(r_i - c_1)^{2(\beta-1)} = R$, $i \in \mathcal{S}$ and $(\eta_1, \ldots, \eta_n)$ is a global maximum of $\mathcal{L}_{\mathbb{T}}$. With these assumptions ($d = 2$) we analyze the maxima of $\mathcal{L}_{\mathbb{T}}$.

Proposition 2.2: The following statements hold true.

(i) The point $(\eta_1, \ldots, \eta_n) \in \mathbb{T}^n$ is a critical point for $\mathcal{L}_{\mathbb{T}}$ if and only if either

$$\sum_{i \in \mathcal{S}} \cos 2\eta_i = 0\,, \qquad \sum_{i \in \mathcal{S}} \sin 2\eta_i = 0,$$

or any two vectors in $\{(\cos 2\eta_i, \sin 2\eta_i)\}_{i \in \mathcal{S}}$, are aligned.

(ii) $\max \mathcal{L}_{q_0} = \max \mathcal{L}_{\mathbb{T}} = \frac{\beta^4 R^2}{4\sigma^2} n_{\mathcal{S}}$, where $n_{\mathcal{S}} = |\mathcal{S}|$.

(iii) For $n_{\mathcal{S}} = |\mathcal{S}|$, define $\eta_{i_s} = (s-1)\pi/n$, and $\eta'_{i_s} = (s-1)2\pi/n$, where $i_s \in \mathcal{S}$, and $s \in \{1, \ldots, n_{\mathcal{S}}\}$. Then, $\{(\eta_1 + k_1\pi, \ldots, \eta_n + k_n\pi) \,|\, k_1, \ldots, k_n \in \mathbb{Z}\} \cup \{(\eta'_1 + k_1\pi, \ldots, \eta'_n + k_n\pi) \,|\, k_1, \ldots, k_n \in \mathbb{Z}\}$ are global maxima for $\mathcal{L}_{\mathbb{T}}$.

We refer to Appendix B for a proof.

Remark 2.3: Due to the periodicity of $\mathcal{L}_{\mathbb{T}}$ for $T = \pi$, there also are global maximum with multiple sensors at the same position. This could be a consequence of our assumptions that the measurement noises w_j are uncorrelated. It is a conjecture that, if the w_j depended on the sensors

locations, then coincident locations could not be part of the set of maximum points. •

III. Decentralized motion coordination for the non-random parameter scenario

In this section we present a family of decentralized control laws that steers the sensors locations to a set of points of maximum for the cost functions discussed in the previous section. Our analysis methods are related to the approaches in [7], [8], [9]. We make the following assumptions on the agents' motion, sensing, and communication:

(i) a static target q_0 belongs to the interior of a compact convex set Q with boundary ∂Q;
(ii) the measurement model is the one described in equation (1) with $h(r) = r$, i.e., equation (6) with $\gamma = 1$, $\beta = 1$, $c_1 = c_2 = 0$, $R_0 = 0$, $R_1 = +\infty$;
(iii) each of the sensors $\{p_1, \ldots, p_n\}$ moves in discrete time in an unbounded fashion along ∂Q;
(iv) each of the sensors $\{p_1, \ldots, p_n\}$ detects its immediate clockwise and counterclockwise neighbors in ∂Q and knows its relative position along ∂Q.

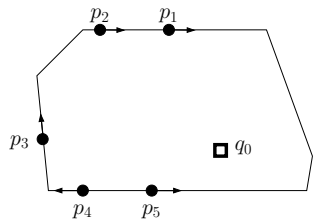

Fig. 1. Assumptions (i) and (iii): the sensors move along the boundary of Q and the target moves inside Q.

For this non-random parameter estimation scenario with limited information, the motion coordination objective is to steer $\{p_1, \ldots, p_n\}$ to the equally-spaced angle positions around the target q_0 exponentially fast.

Remark 3.1:

- Assumptions (ii), (iii) and (iv) could be modified to include an upper bound on the motion and detection range of the sensors; we leave these important extensions to future works (in the interest of brevity).
- Assumption (iv) means that an implementable control law for an agent can only depend on the agent's position relative to its neighbors (in the natural ring topology along ∂Q). We will call such a control law *spatially distributed along* ∂Q.
- We will allow the control law to depend on the current estimate of the target location. This strategy is said to be of the "certainty equivalence" type. •

A. From the boundary of Q to a circle and back

Because we assume that the n sensors can be placed only along the boundary of the convex set Q, we can simplify the design of motion control strategies as follows. Instead of working with the positions $p_1, \ldots, p_n$ in ∂Q, we will work with their polar coordinates centered at q_0, and we will define our motion control algorithms on the circle.

Let us be more formal on this matter. Let ∂Q be implicitly defined by the continuous equation $x \in \partial Q$ if and only if $g(x) = 0$. Given a point q in the interior of a compact convex set Q, define the map $\varphi_q : \partial Q \to \mathbb{T}$ by

$$\varphi_q(p) = \frac{p - q}{\|p - q\|}.$$

One can show that the map φ_q is continuous with continuous inverse $\varphi_q^{-1} : \mathbb{T} \to \partial Q$ given by

$$\varphi_q^{-1}(v) = q + \lambda v,$$

where $\lambda \in \mathbb{R}_+$ the unique solution to $g(q + \lambda p) = 0$.

In what follows, we let q_0 denote the current estimate of the target location and $\varphi_{q_0}(p)$ be the angular component of the polar coordinates centered at q_0. In summary, we can identify $p_i \in \partial Q \subset \mathbb{R}^2$ with $\eta_i = \varphi_{q_0}(p_i) \in \mathbb{T}$, for $i \in \{1, \ldots, n\}$.

B. Two basic behaviors for uniform coverage of the circle

As discussed, the location of the sensors is described by the vector $(\eta_1, \ldots, \eta_n)$ of elements of $\mathbb{T}$. We assume that angles are measured counterclockwise and that the sensors are placed in counterclockwise order (we adopt the convention that $\eta_{n+1} = \eta_1$ and that $\eta_0 = \eta_n$).

The motion of the sensors is described by a discrete-time control system:

$$\eta_i(k+1) = \eta_i(k) + u_i, \quad i \in \{1, \ldots, n\}.$$

Here u_i is the scalar control magnitude of the ith sensor. The control can depend only the measurement and communication available to the sensor, i.e., u_i is a function only of the relative angular distances in the counterclockwise direction $d_{\text{counter-clock},i} = \eta_{i+1} - \eta_i > 0$ and clockwise direction $d_{\text{clock},i} = \eta_i - \eta_{i-1} > 0$. We also assume that each sensor obeys the same motion control law $u : [0, 2\pi] \times [0, 2\pi] \to \mathbb{R}$, so that the closed-loop system will be

$$\begin{aligned} \eta_i(k+1) &= \eta_i(k) + u(d_{\text{counterclock},i}(k), d_{\text{clock},i}(k)), \\ d_{\text{counterclock},i}(k) &= \eta_{i+1}(k) - \eta_i(k), \\ d_{\text{clock},i}(k) &= \eta_i(k) - \eta_{i-1}(k). \end{aligned}$$

In order to achieve uniform distribution of the sensors on the circle, two simple behaviors arise fairly naturally, see Figure 2. First, we consider the Go towards the midpoint behavior $u_{\text{midpoint}} : [0, 2\pi] \times [0, 2\pi] \to \mathbb{R}$ given by:

$$u_{\text{midpoint}}(d_{\text{counterclock}}, d_{\text{clock}}) = \frac{1}{2}\big(d_{\text{counterclock}} - d_{\text{clock}}\big).$$

The interpretation is clear: each sensor moves towards the midpoint of the angular segment between the preceding and following sensor. In the original coordinate system, each sensor moves along ∂Q towards the bisector of the triangle with vertex q_0 and vertices given by the preceding and following sensor.

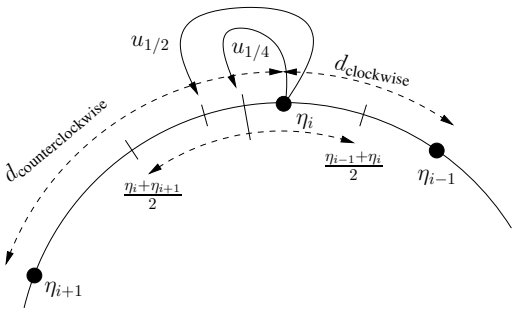

Fig. 2. The GO TOWARDS THE MIDPOINT $u_{1/2}$ and GO TOWARDS THE MIDPOINT OF VORONOI SEGMENT $u_{1/4}$ behaviors.

A second intuitive rule is the GO TOWARDS THE MIDPOINT OF VORONOI SEGMENT behavior $u_{\text{midpoint Voronoi}} : [0, 2\pi] \times [0, 2\pi] \to \mathbb{R}$ given by:

$$u_{\text{midpoint Voronoi}}(d_{\text{counterclock}}, d_{\text{clock}}) = \frac{1}{4}\big(d_{\text{counterclock}} - d_{\text{clock}}\big).$$

The interpretation is the following: the Voronoi segment of the ith sensor at position η_i is the angular segment from $(\eta_{i-1} + \eta_i)/2$ to $(\eta_i + \eta_{i+1})/2$, and the control law GO TOWARDS THE MIDPOINT OF VORONOI SEGMENT steers η_i towards the midpoint of this segment.

These two rules are particular instances of the following family of linear algorithms parametrized by $\mathcal{K} \in \mathbb{R}$:

$$u_{\mathcal{K}}(d_{\text{counterclock}}, d_{\text{clock}}) = \mathcal{K}(d_{\text{counterclock}} - d_{\text{clock}}).$$

Clearly, u_{midpoint} and $u_{\text{midpoint Voronoi}}$ are equal to $u_{\mathcal{K}}$ for $\mathcal{K} = 1/2$ and $\mathcal{K} = 1/4$, respectively. Because $u_{\mathcal{K}}(d, d) = 0$ for all $d \in \mathbb{R}_+$, the equally-spaced angle position (where the sensors are uniformly distributed around the target) is an equilibrium point[3] for the $u_{\mathcal{K}}$-closed-loop system.

C. Convergence analysis

To perform a convergence analysis, it is convenient to define the relative angular distances $d_i = \eta_{i+1} - \eta_i$, for $i \in \{1, \dots, n\}$ (and adopt the usual convention that $d_{n+1} = d_1$ and that $d_0 = d_n$). So long as the counterclockwise order of the sensors is not violated, we have $(d_1, \dots, d_n) \in S_{2\pi} = \{x \in \mathbb{R}_n \mid x_i \geq 0, \sum_{i=1}^n x_i = 2\pi\}$. The change of coordinates from $(\eta_1, \dots, \eta_n)$ to $(d_1, \dots, d_n)$ and the control law $u_{\mathcal{K}}$ jointly lead to the closed-loop system

$$d_i(k+1) = \mathcal{K}d_{i+1}(k) + (1 - 2\mathcal{K})d_i(k) + \mathcal{K}d_{i-1}(k).$$

This is a linear time-invariant dynamical system with state $d = (d_1, \dots, d_n)$, transition matrix $A_{\mathcal{K}}$ given by

$$\begin{bmatrix} 1-2\mathcal{K} & \mathcal{K} & \cdots & \mathcal{K} \\ \mathcal{K} & 1-2\mathcal{K} & \cdots & 0 \\ \vdots & \ddots & \ddots & \vdots \\ \mathcal{K} & 0 & \mathcal{K} & 1-2\mathcal{K} \end{bmatrix},$$

[3]The more general linear feedback $u(d_{\text{counterclock}}, d_{\text{clock}}) = ad_{\text{counterclock}} + bd_{\text{clock}}$ does not have the desired equilibrium set unless $a + b = 0$. The case of $a + b \neq 0$ is studied in the context of cyclic pursuit, see [7] and references therein.

and governing equation

$$d(k+1) = A_{\mathcal{K}}d(k), \quad \text{for } k \in \mathbb{N} \cup \{0\}. \tag{7}$$

Theorem 3.2: The control law $u_{\mathcal{K}}$ is spatially distributed along ∂Q, and, for $\mathcal{K} \in]0, 1/2[$, the solutions to the corresponding closed-loop system (7) preserve the counterclockwise order of the sensors and converge exponentially fast to $(2\pi/n, \dots, 2\pi/n)$.

Recall the notion and properties of circulant matrices from Appendix C. Note that $A_{\mathcal{K}}$ is circulant with representer $p_{A_{\mathcal{K}}}(s) = (1 - 2\mathcal{K}) + \mathcal{K}s + \mathcal{K}s^{n-1}$. Theorem A.1 implies that the eigenvalues of $A_{\mathcal{K}}$ are

$$\lambda_\ell = p_{A_{\mathcal{K}}}\Big(\exp\big(\frac{2\pi\ell\sqrt{-1}}{n}\big)\Big) = 1 - 2\mathcal{K} + 2\mathcal{K}\cos\big(\frac{2\pi\ell}{n}\big),$$

for $\ell \in \{1, \dots, n\}$. It is easy to see that $\lambda_n = 1$ and that the corresponding eigenvector is $\mathbf{1}^T = (1, \dots, 1)$. If $\mathcal{K} > 0$ and $\ell \in \{1, \dots, n-1\}$, then

$$-1 \leq \cos\big(\frac{2\pi\ell}{n}\big) < 1 \quad \Longrightarrow \quad 1 - 4\mathcal{K} \leq \lambda_\ell < 1.$$

Therefore, if $\mathcal{K} \in]0, 1/2[$, then the eigenvalues $\lambda_1, \dots, \lambda_{n-1}$ belong to the open interval $]-1, 1[$. Additionally, if $\mathcal{K} \in]0, 1/2[$, then $A_{\mathcal{K}}$ is a doubly-stochastic matrix, so that $S_{2\pi}$ is invariant for $A_{\mathcal{K}}$.

Let $\{\mathbf{e}_1, \cdots, \mathbf{e}_{n-1}, \mathbf{1}\}$ be a basis of orthogonal eigenvectors for $A_{\mathcal{K}}$ corresponding to the eigenvalues $\{\lambda_1, \dots, \lambda_n\}$, respectively. Any initial condition $d(0)$ satisfies

$$d(0) = \sum_{\ell=1}^{n-1} \rho_\ell \mathbf{e}_\ell + \rho_n \mathbf{1}\,.$$

Since $\sum_{i=1}^n d_i(0) = 2\pi$, we have that

$$2\pi = \mathbf{1}^T d(0) = \rho_n \mathbf{1}^T \mathbf{1} = \rho_n n \quad \Longrightarrow \quad \rho_n = \frac{2\pi}{n}\,.$$

On the other hand,

$$d(k) = A_{\mathcal{K}}d(k-1) = \sum_{\ell=1}^{n-1} \lambda_\ell^k \rho_\ell\, \mathbf{e}_\ell + \rho_n \mathbf{1}\,.$$

If $\mathcal{K} \in]0, 1/2[$, then each $|\lambda_\ell| < 1$, for $\ell \in \{1, \dots, n-1\}$ and, therefore, each trajectory $k \mapsto d(k)$ converges to $\rho_n \mathbf{1}$, the equal-angle configuration, exponentially fast.

Remark 3.3:

(i) The properties of $u_{\mathcal{K}}$ in Theorem 3.2 are independent of the number n of sensors.

(ii) If $\mathcal{K} < 0$ or $\mathcal{K} > 1/2$, then there exist initial conditions from which the counterclockwise order of the sensors is not preserved in the closed loop.

(iii) Consider the $\mathcal{K} = 1/2$ case, corresponding to the GO TOWARDS THE MIDPOINT behavior. Although GO TOWARDS THE MIDPOINT is a very natural algorithm to consider, it does *not* ensure convergence to the desired configuration whenever n is even. In fact, if $n = 2L$ with $L \in \mathbb{Z}$, then $\mathbf{1}$ and $\mathbf{e}_L^T = (-1, 1, -1, \dots, -1, 1)$ are eigenvectors with eigenvalues 1 and -1 respectively. Given $\{\mathbf{e}_1 \dots, \mathbf{e}_{n-1}, \mathbf{1}\}$ an orthogonal basis of eigenvectors for $A_{1/2}$ and $d(0) = \sum_{i=1}^{n-1} \rho_i \mathbf{e}_i + \rho_n \mathbf{1}$, one can

show that the system will exponentially converge to a steady oscillation between $\mathbf{u}_1 = \rho_n \mathbf{1} + \rho_L \mathbf{e}_L$ and $\mathbf{u}_2 = \rho_n \mathbf{1} - \rho_L \mathbf{e}_L$. •

IV. Target tracking simulations with Kalman filtering and motion coordination algorithms

Here we combine the developments of former sections to define the Active Target Tracking algorithm for collective improved sensing performance. We numerically simulate the algorithm to validate our approach. It is assumed that the estimation step is carried out after a round of communication has taken place to propagate all the measurements taken among the agents[4]. The algorithm is summarized in the following table.

Name:	Active Target Tracking Algorithm
Goal:	Decentralized motion coordination of sensors and joint localization of target
Data:	(i) Constant $\mathcal{K} \in]0, 1/2[$. (ii) Equation for the boundary of the containment region, $g(q) = 0$. (iii) Initial guess for the target initial position $\hat{q}_0(0)$.

At time k, local agent $i \in \{1, \ldots, n\}$ performs:

1: Receive estimate $\hat{q}_0(k)$ from fusion center.
2: Detect counterclockwise and clockwise neighbors along ∂Q, compute angular distances in polar coordinates about $\hat{q}_0(k)$.
3: Compute control $u_{\mathcal{K}}$, next desired position $\eta_i(k+1) \in \mathbb{T}$, and corresponding point $p_i(k+1) \in \partial Q$.
4: Move to new position $p_i(k+1)$ along ∂Q.
5: Take new measurement of target $z_i(k+1)$, and send it to fusion center, that will update target estimate according to EKF.

In what follows we present our numerical results. we compare the estimation errors of the trajectory of a dynamic target obtained from a set of four stationary and moving sensors. For the purpose of the simulation, Q will be a ball centered at the origin with radius $1.5m$, and the trajectory or the target will be the eight-shaped curve:

$$\begin{bmatrix} q_0^1(k) \\ q_0^2(k) \end{bmatrix} = \begin{bmatrix} \sin(\omega k) \\ \sin(\omega k)\cos(\omega k) \end{bmatrix}, \qquad k \geq 0\,.$$

Here (q_0^1, q_0^2) are measured in meters and $\omega = .1$ rad/sec.

In all the subsequent figures, the plots compares the evolution of the absolute error trajectories along time, $E(k) = \|q_0(k) - \hat{q}_0(k)\|$ for stationary sensors (solid blue line) and moving sensors (dashed red line), for $k \geq 0$.

The first set of simulations, Figure 3, reproduce the results obtained for four sensors initially positioned at 2.1818, 2.4500, 3.7160, and 4.5167 radians. As can be seen, the moving sensors perform better on average as the variance increases. In the second set of simulations, Figure 4, we take as the initial position for the sensors the optimal position to estimate $\mathbf{0}$. That is, 0, $\pi/2$, π and $3\pi/2$,

[4]This would be equivalent as having a fusion center that centralizes the estimation process

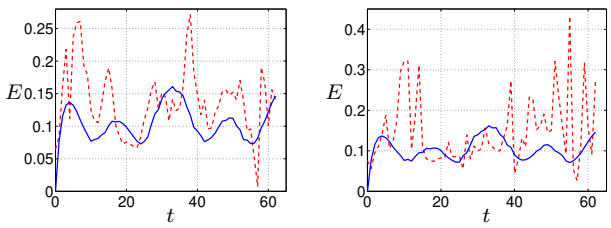

Fig. 3. Evolution of absolute error trajectories with variances of measured noise 5×10^{-3} (left) and 5×10^{-2} (right).

are the initial positions for both stationary and moving sensors. Though the set of moving sensors performs better,

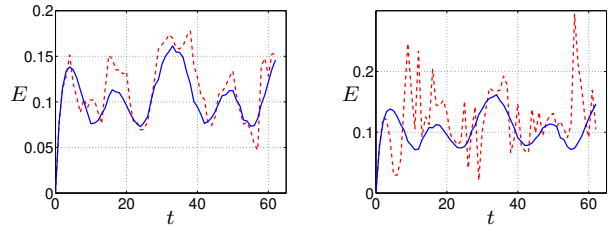

Fig. 4. Evolution of absolute error trajectories with variances of measured noise 5×10^{-3} (left) and 10^{-1} (right).

the differences between the estimates of the stationary and moving sensors are comparable for variances of order 10^{-4}, 10^{-3} (the absolute error trajectories overlap) and even not so different when the variances are increased to order 10^{-2}. One has to increase the order of noise to 10^{-1} to observe a clear difference in performance. Qualitatively, Figure 5 shows how the estimated trajectories of the moving sensors (green solid line) behaves compared with the estimation provided by the stationary sensors (black dashed line). The green solid trajectory is very close to the actual trajectory of the target that we do not plot. Note that in all the simulations, the variance of the process noise is kept minimum of order 10^{-5}. It can be observed in the simulations that when the variance of the measurement is kept constant and the variance of the process noise is varied, both performances of stationary and moving sensors give very similar results.

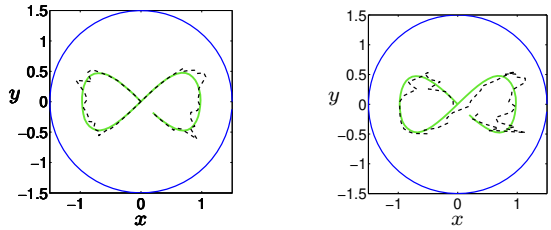

Fig. 5. Qualitative evolution of the estimated trajectories by moving and stationary sensors. Initial positions are $(0, \pi/2, \pi, 3\pi/2)$ (left) and $(2.1818, 2.4500, 3.7160, 4.5167)$ (right) and variances are in both cases 5×10^{-2}.

V. Conclusions and future work

We have presented novel decentralized control laws for the optimal positioning of sensor networks that track a target. Future research lines include (1) the consideration of heterogeneous collections of sensors, (2) the dynamic assignment of sensors to different targets and (3) investigation of decentralized estimation and fusion schemes.

Acknowledgement

This material is based upon work supported in part by ONR YIP Award N00014-03-1-0512 and NSF SENSORS Award IIS-0330008. Sonia Martínez's work was partially supported by a Fulbright Postdoctoral Fellowship from the Spanish Ministry of Education and Culture.

References

[1] T. Mukai and M. Ishikawa, "An active sensing method using estimated errors for multisensor fusion systems," *IEEE Transactions on Industrial Electronics*, vol. 43, no. 3, pp. 380–386, 1996.

[2] C. S. Kubrusly and H. Malebranche, "Sensors and controllers location in distributed systems–a survey," *Automatica*, vol. 21, no. 2, pp. 117–128, 1985.

[3] B. Porat and A. Nehorai, "Localizing vapor-emitting sources by moving sensors," *IEEE Transactions on Signal Processing*, vol. 44, no. 4, pp. 1018–1021, 1996.

[4] T. H. Chung, V. Gupta, J. W. Burdick, and R. M. Murray, "On a decentralized active sensing strategy using mobile sensor platforms in a network," in *IEEE Conf. on Decision and Control*, Paradise Island, Bahamas, 2004, pp. 1914–1919.

[5] D. Uciński, "Optimal sensor location for parameter estimation of distributed processes," *International Journal of Control*, vol. 73, no. 13, pp. 1235–48, 2000.

[6] E. Rafajlowicz, "Optimum choice of moving sensor trajectories for distributed-parameter system identification," *International Journal of Control*, vol. 43, no. 5, pp. 1441–51, 1986.

[7] J. A. Marshall, M. E. Broucke, and B. A. Francis, "Formations of vehicles in cyclic pursuit," *IEEE Transactions on Automatic Control*, vol. 49, no. 11, pp. 1963–1974, 2004.

[8] A. Jadbabaie, J. Lin, and A. S. Morse, "Coordination of groups of mobile autonomous agents using nearest neighbor rules," *IEEE Transactions on Automatic Control*, vol. 48, no. 6, pp. 988–1001, 2003.

[9] R. Olfati-Saber and R. M. Murray, "Consensus problems in networks of agents with switching topology and time-delays," *IEEE Transactions on Automatic Control*, vol. 49, no. 9, pp. 1520–1533, 2004.

[10] B. S. Y. Rao, H. F. Durrant-Whyte, and J. S. Sheen, "A fully decentralized multi-sensor system for tracking and surveillance," *International Journal of Robotics Research*, vol. 12, no. 1, pp. 20–44, 1993.

[11] A. G. O. Mutambara, *Decentralized Estimation and Control for Multisensor Systems*. CRC Press, 1998.

[12] D. L. Hall and J. Llinas, "An introduction to multisensor data fusion," *Proceedings of the IEEE*, vol. 85, no. 1, pp. 6–23, 1997.

[13] B. Sinopoli, L. Schenato, M. Franceschetti, K. Poolla, M. I. Jordan, and S. S. Sastry, "Kalman filtering with intermittent observations," *IEEE Transactions on Automatic Control*, vol. 49, no. 9, pp. 1453–1463, 2004.

[14] Y. Bar-Shalom, X. R. Li, and T. Kirubarajan, *Estimation with Applications to Tracking and Navigation*. John Wiley & Sons, 2001.

[15] D. Uciński, "Optimal selection of measurement locations for parameter estimation in distributed processes," *International Journal of Applied Mathematics and Computer Science*, vol. 10, no. 2, pp. 357–79, 2000.

[16] P. J. Davis, *Circulant Matrices*, 2nd ed. American Mathematical Society, 1994.

[17] R. A. Horn and C. R. Johnson, *Matrix Analysis*. Cambridge University Press, 1985.

Appendix

A. Proof of Proposition 2.1

(i) Let $d = 2$. The determinant of J_{NR} is computed as follows:

$$\begin{aligned}
&\sigma^2 \det J_{\text{NR}} = \\
&\left(\sum_{i=1}^{n}(\partial_1 h_i)^2\right)\left(\sum_{j=1}^{n}(\partial_2 h_j)^2\right) - \left(\sum_{i=1}^{n}\partial_1 h_i\, \partial_2 h_i\right)^2 \\
&= \sum_{i=1}^{n}(\partial_1 h_i)^2(\partial_2 h_i)^2 + \sum_{\substack{i,\,j\,=\,1\\ i\,\neq\, j}}^{n}(\partial_1 h_i)^2(\partial_2 h_j)^2 - \\
&\left(\sum_{i=1}^{n}(\partial_1 h_i)^2(\partial_2 h_i)^2 + \sum_{\substack{i,\,j\,=\,1\\ i\,\neq\, j}}^{n}\partial_1 h_i\, \partial_2 h_i\, \partial_1 h_j\, \partial_2 h_j\right) \\
&= \sum_{\substack{i,\,j\,=\,1\\ i\,\neq\, j}}^{n}\left((\partial_1 h_i)^2(\partial_2 h_j)^2 - \partial_1 h_i\, \partial_2 h_i\, \partial_1 h_j\, \partial_2 h_j\right) \\
&= \sum_{\substack{i,\,j\,=\,1\\ i\,\leq\, j}}^{n}\left((\partial_1 h_i)^2(\partial_2 h_j)^2 + (\partial_1 h_j)^2(\partial_2 h_i)^2\right) \\
&\qquad\qquad - 2\sum_{\substack{i,\,j\,=\,1\\ i\,\leq\, j}}^{n}\partial_1 h_i\, \partial_2 h_i\, \partial_1 h_j\, \partial_2 h_j \\
&= \sum_{\substack{i,\,j\,=\,1\\ i\,\leq\, j}}^{n}\left(\partial_1 h_i\, \partial_2 h_j\ - \partial_2 h_i\, \partial_1 h_j\right).
\end{aligned}$$

If we set $\mathbf{v}_i = (\partial_1 h_i, \partial_2 h_i, 0)$, $i \in \{1, \ldots, n\}$, then clearly,

$$\begin{aligned}
&\det J_{\text{NR}} = \\
&\frac{1}{\sigma^2}\sum_{\substack{i,\,j\,=\,1\\ i\,\leq\, j}}^{n}\left((\mathbf{v}_i \times \mathbf{v}_j)\cdot(0,0,1)\right)^2 = \frac{1}{\sigma^2}\sum_{\substack{i,\,j\,=\,1\\ i\,\leq\, j}}^{n}\|\mathbf{v}_i \times \mathbf{v}_j\|^2 \\
&= \frac{1}{\sigma^2}\sum_{\substack{i,\,j\,=\,1\\ i\,\leq\, j}}^{n}\|\mathbf{v}_i\|^2\|\mathbf{v}_j\|^2 \sin^2\alpha_{ij} = \frac{1}{2\sigma^2}\sum_{i,j=1}^{n}\|\mathbf{v}_i \times \mathbf{v}_j\|^2.
\end{aligned}$$

Here $\|\mathbf{v}_i \times \mathbf{v}_j\|$ represents the area of the parallelogram generated by $\mathbf{v}_i$ and $\mathbf{v}_j$.

(ii) Let $d = 3$. From the formula for the determinant of J_{NR} we obtain

$$\begin{aligned}
&\sigma^2 \det J = \\
&\sum_{i,j,k=1}^{n}\partial_1 h_i\, \partial_2 h_j\, \partial_3 h_k\Big(\partial_1 h_i\, \partial_2 h_j\, \partial_3 h_k + \\
&\partial_1 h_k\, \partial_2 h_i\, \partial_3 h_j + \partial_1 h_j\, \partial_2 h_k\, \partial_3 h_i - \partial_1 h_k\, \partial_2 h_j\, \partial_3 h_i \\
&- \partial_1 h_i\, \partial_2 h_k\, \partial_3 h_j - \partial_1 h_j\, \partial_2 h_i\, \partial_3 h_k\Big).
\end{aligned}$$

Observe that this expression reduces to

$$\sigma^2 \det J = \sum_{i,j,k=1}^{n}\partial_1 h_i\, \partial_2 h_j\, \partial_3 h_k\left[(\mathbf{v}_i \times \mathbf{v}_j)\cdot \mathbf{v}_k\right],$$

with $\mathbf{v}_i \triangleq (\partial_1 h_i, \partial_2 h_i, \partial_3 h_i)$, for $i \in \{1, \ldots, n\}$.

We can further simplify the determinant as follows:

$$\sum_{i,j,k=1}^{n} \partial_1 h_i\, \partial_2 h_j\, \partial_3 h_k\, [(\mathbf{v}_i \times \mathbf{v}_j) \cdot \mathbf{v}_k] =$$

$$= \sum_{\substack{i,\,j,\,k\,=\,1 \\ i\,\le\,j}}^{n} \partial_1 h_i\, \partial_2 h_j\, \partial_3 h_k\, [(\mathbf{v}_i \times \mathbf{v}_j) \cdot \mathbf{v}_k] + \sum_{\substack{i,\,j,\,k\,=\,1 \\ j\,\le\,i}}^{n} \partial_1 h_i\, \partial_2 h_j\, \partial_3 h_k\, [(\mathbf{v}_i \times \mathbf{v}_j) \cdot \mathbf{v}_k]$$

$$= \sum_{\substack{i,\,j,\,k\,=\,1 \\ i\,\le\,j}}^{n} \partial_3 h_k\, [\partial_1 h_i\, \partial_2 h_j - \partial_1 h_j\, \partial_2 h_i]\, (\mathbf{v}_i \times \mathbf{v}_j) \cdot \mathbf{v}_k\,.$$

The last summand can be split into two as

$$\sum_{\substack{i,\,j,\,k\,=\,1 \\ i\,\le\,j}}^{n} = \sum_{\substack{i,\,j,\,k\,=\,1 \\ i\,\le\,j\,\le\,k}}^{n} + \sum_{\substack{i,\,j,\,k\,=\,1 \\ i,\,k\,\le\,j}}^{n}\,,$$

now, rewriting the second of these terms as

$$\sum_{\substack{i,\,j,\,k\,=\,1 \\ i,\,k\,\le\,j}}^{n} \partial_3 h_k\, [\partial_1 h_i \partial_2 h_j - \partial_1 h_j \partial_2 h_i]\, (\mathbf{v}_i \times \mathbf{v}_j) \cdot \mathbf{v}_k =$$

$$\sum_{\substack{i,\,j,\,k\,=\,1 \\ k\,\le\,i\,\le\,j}}^{n} \partial_3 h_k\, [\partial_1 h_i \partial_2 h_j - \partial_1 h_j \partial_2 h_i]\, (\mathbf{v}_i \times \mathbf{v}_j) \cdot \mathbf{v}_k +$$

$$\sum_{\substack{i,\,j,\,k\,=\,1 \\ i\,\le\,k\,\le\,j}}^{n} \partial_3 h_k\, [\partial_1 h_i \partial_2 h_j - \partial_1 h_j \partial_2 h_i]\, (\mathbf{v}_i \times \mathbf{v}_j) \cdot \mathbf{v}_k =$$

$$\sum_{\substack{i,\,j,\,k\,=\,1 \\ i\,\le\,j\,\le\,k}}^{n} \partial_3 h_i\, [\partial_1 h_j \partial_2 h_k - \partial_1 h_k \partial_2 h_j]\, (\mathbf{v}_j \times \mathbf{v}_k) \cdot \mathbf{v}_i +$$

$$\sum_{\substack{i,\,j,\,k\,=\,1 \\ i\,\le\,j\,\le\,k}}^{n} \partial_3 h_j\, [\partial_1 h_i \partial_2 h_k - \partial_1 h_k \partial_2 h_i]\, (\mathbf{v}_i \times \mathbf{v}_k) \cdot \mathbf{v}_j\,,$$

and using that $(\mathbf{v}_j \times \mathbf{v}_k) \cdot \mathbf{v}_i$ are invariant under cyclic permutations of i, j and $k \in \{1, \dots, n\}$, we obtain:

$$\sigma^2 \det J = \sum_{i \le j \le k} \Big(\partial_3 h_k\, [\partial_1 h_i\, \partial_2 h_j - \partial_1 h_j\, \partial_2 h_i] + \partial_3 h_i\, [\partial_1 h_j\, \partial_2 h_k - \partial_1 h_k\, \partial_2 h_j] + \partial_3 h_j\, [\partial_1 h_k\, \partial_2 h_i - \partial_1 h_i\, \partial_2 h_k] \Big) (\mathbf{v}_i \times \mathbf{v}_j) \cdot \mathbf{v}_k\,.$$

This expression is equivalent to:

$$\det J = \frac{1}{\sigma^2} \sum_{i \le j \le k} |(\mathbf{v}_i \times \mathbf{v}_j) \cdot \mathbf{v}_k|^2 = \frac{1}{\sigma^2} \sum_{i \le j \le k} \|\mathbf{v}_i\|^2 \|\mathbf{v}_j\|^2 \|\mathbf{v}_k\|^2 \sin^2 \alpha_{ij} \cos^2 \beta_{ij,k}\,,$$

where $\alpha_{ij} = \measuredangle(\mathbf{v}_i, \mathbf{v}_j)$, and $\beta_{ij,k} = \measuredangle(\mathbf{v}_i \times \mathbf{v}_j, \mathbf{v}_k)$. Here, $|(\mathbf{v}_i \times \mathbf{v}_j) \cdot \mathbf{v}_k|$ has the interpretation of the volume generated by the vectors $\mathbf{v}_i$, $\mathbf{v}_j$ and $\mathbf{v}_j$. We get in this way an analogous formula to that of $d = 2$. As in the two-dimensional case, it is easy to see that

$$\det J = \frac{1}{6\,\sigma^2} \sum_{i,j,k} |(\mathbf{v}_i \times \mathbf{v}_j) \cdot \mathbf{v}_k|^2\,.$$

B. Proof of Proposition 2.2

In first place, since $\mathcal{L}_{\mathbb{T}}$ is differentiable, $(\eta_1, \dots, \eta_n)$ is a critical point of $\mathcal{L}_{\mathbb{T}}$ if and only if

$$\frac{\partial}{\partial \eta_k} \sum_{i,j \in \mathcal{S}} \sin^2(\eta_i - \eta_j) = 0\,, \quad \forall k \in \{1, \dots, n\}\,.$$

In other words, for all $k \in \mathcal{S}$ we have

$$0 = \sum_{i \in \mathcal{S}} \sin[2(\eta_k - \eta_i)] = \sin 2\eta_k \sum_{i \in \mathcal{S}} \cos 2\eta_i - \cos 2\eta_k \sum_{i \in \mathcal{S}} \sin 2\eta_i = \Big((\cos 2\eta_k, \sin 2\eta_k, 0) \times \sum_{i \in \mathcal{S}} (\cos 2\eta_i, \sin 2\eta_i, 0) \Big) \cdot \mathbf{e}_3.$$

This equality holds if (1) two vectors $(\cos 2\eta_k, \sin 2\eta_k, 0)$ are all aligned, $k \in \mathcal{S}$, and perpendicular to the non-zero vector $\mathbf{x} = \sum_{i \in \mathcal{S}} (\cos 2\eta_i, \sin 2\eta_i, 0)$, or (2) $\sum_{i \in \mathcal{S}} (\cos 2\eta_i, \sin 2\eta_i, 0) = 0$. That is, $(\eta_1, \dots, \eta_n)$ is a critical point for $\mathcal{L}_{\mathbb{T}}$ if and only if

$$\sum_{i \in \mathcal{S}} \cos 2\eta_i = 0\,, \qquad \sum_{i \in \mathcal{S}} \sin 2\eta_i = 0\,, \tag{8}$$

or any two vectors in $\{(\cos 2\eta_i, \sin 2\eta_i)\}_{i \in \mathcal{S}}$, are aligned.

Secondly, since $\mathcal{L}_{\mathbb{T}}$ is differentiable and its domain is open, its global maxima are contained in the set of its critical points. Therefore, we will focus on the valuation of $\mathcal{L}_{\mathbb{T}}$ on critical points.

Let a_{ij} denote $a_{ij} = |\eta_i - \eta_j|$. We have that

$$\sum_{i,j \in \mathcal{S}} \sin^2(\eta_i - \eta_j) = \sum_{i,j \in \mathcal{S}} \sin^2 a_{ij}\,.$$

Taking complex exponentials, we compute

$$2 \sum_{i,j \in \mathcal{S}} \sin^2 a_{ij} = 2 \sum_{i,j \in \mathcal{S}} \left(\frac{\mathrm{e}^{\mathbf{i} a_{ij}} - \mathrm{e}^{-\mathbf{i} a_{ij}}}{2\mathbf{i}} \right)^2 \sum_{i,j \in \mathcal{S}} \left(\frac{\mathrm{e}^{2\mathbf{i} a_{ij}} + \mathrm{e}^{-2\mathbf{i} a_{ij}} - 2}{-2} \right) = n_{\mathcal{S}}^2 - \sum_{i,j \in \mathcal{S}} \cos 2a_{ij}\,,$$

where $\mathbf{i} = \sqrt{-1}$. Using now the formula for the cosine of a sum, we obtain:

$$\sum_{i,j \in \mathcal{S}} \cos 2a_{ij} = \sum_{i,j \in \mathcal{S}} \cos 2(\eta_i - \eta_j) = \sum_{i,j \in \mathcal{S}} \cos 2\eta_i \cos 2\eta_j + \sin 2\eta_i \sin 2\eta_j = \sum_{i \in \mathcal{S}} \cos 2\eta_i \sum_{j \in \mathcal{S}} \cos 2\eta_j + \sum_{i \in \mathcal{S}} \sin 2\eta_i \sum_{j \in \mathcal{S}} \sin 2\eta_j\,.$$

Therefore, at critical points for which (8) holds, we have that

$$2\sum_{i,j\in\mathcal{S}}\sin^2 a_{ij} = n_{\mathcal{S}}^2\,.$$

Consider now the critical points $(\eta_1,\dots,\eta_n)$ such that any two vectors in $\{(\cos 2\eta_i,\sin 2\eta_i)\}_{i\in\mathcal{S}}$ are aligned. Let n_1 be the cardinal of the set N_1 of vectors that coincide with $(\cos\eta_{i_1},\sin\eta_{i_1})$ and let n_2 be the cardinal of the set N_2 of vectors which are perpendicular to $(\cos\eta_{i_1},\sin\eta_{i_1})$, for some $i_1\in\mathcal{S}$. We have that

$$\begin{aligned}2\sum_{i,j\in\mathcal{S}}\sin^2 a_{ij} &= 2\sum_{i\in N_1,j\in N_2}\sin^2 a_{ij} + 2\sum_{i\in N_2,j\in N_1}\sin^2 a_{ij}\\ &= 2n_1n_2 + 2n_2n_1 = 4n_1n_2\,,\end{aligned}$$

But $4n_1n_2\le(n_1+n_2)^2 = n_{\mathcal{S}}^2$, since this is equivalent to $(n_1-n_2)^2\ge 0$. This allows us to say that

$$\mathcal{L}_{q_0}(p_1,\dots,p_n) = \mathcal{L}_{\mathbb{T}}(\eta_1,\dots,\eta_n) \le \frac{\beta^4R^2}{4\sigma^2}n_{\mathcal{S}}\,,$$

for any critical point $(\eta_1,\dots,\eta_n)$ of $\mathcal{L}_{\mathbb{T}}$ and $(p_1,\dots,p_n)$ such that $\beta^2 r_i^{2(\beta-1)} = R$, $i\in\mathcal{S}$.

To prove the third fact of the proposition, consider $x_0 = \mathrm{e}^{\mathbf{i}\frac{2\pi}{n_{\mathcal{S}}}}$. Since $x_0\neq 1$, x_0 must be a root of $p(x)$ where

$$p(x) = x^{n-1}+x^{n-2}+\cdots+x+1\,,\; p(x)(x-1) = x^n-1\,.$$

But this means

$$p(x_0) = \mathrm{e}^{\mathbf{i}\frac{2\pi}{n_{\mathcal{S}}}(n_{\mathcal{S}}-1)} + \mathrm{e}^{\mathbf{i}\frac{2\pi}{n_{\mathcal{S}}}(n_{\mathcal{S}}-2)} + \cdots + \mathrm{e}^{\mathbf{i}\frac{2\pi}{n_{\mathcal{S}}}} + 1 = 0\,,$$

which is equivalent to

$$\sum_{i_s\in\mathcal{S}}\cos\frac{2\pi}{n_{\mathcal{S}}}(s-1) = 0\,,\qquad \sum_{i_s\in\mathcal{S}}\sin\frac{2\pi}{n_{\mathcal{S}}}(s-1) = 0\,.$$

Therefore, $(\eta_1,\dots,\eta_n)$ is a critical point of $\mathcal{L}_{\mathbb{T}}$ when $\eta_{i_s} = \frac{\pi}{n_{\mathcal{S}}}(s-1)$, $i_s\in\mathcal{S}$, or $\eta_{i_s} = \frac{2\pi}{n_{\mathcal{S}}}(s-1)$, $i_s\in\mathcal{S}$. Because of the previous analysis, we have $\mathcal{L}_{\mathbb{T}}(\eta_1,\dots,\eta_n) = \frac{n_{\mathcal{S}}^2R}{4\sigma^2}$.

Observe that since $\sin^2 x = \sin^2(-x)$ is periodic of period $T=\pi$, any configuration in

$$\{(\eta_1+k_1\pi,\dots,\eta_n+k_n\pi)\,|\,k_1,\dots,k_n\in\mathbb{Z}\}$$

for $(\eta_1,\dots,\eta_n)$ a maximum, will be another maximum.

C. Circulant matrices

Circulant matrices are an important class of Toeplitz matrices with useful properties and are related to the Discrete Fourier Transform. For a comprehensive treatment of circulant matrices we refer to [16], see also [17].

A matrix $C\in\mathbb{R}^{n\times n}$ is *(right) circulant* if it is of the form

$$C = \begin{bmatrix} c_1 & c_2 & \cdots & c_n\\ c_n & c_1 & \cdots & c_{n-1}\\ \vdots & \ddots & \ddots & \vdots\\ c_2 & c_3 & \cdots & c_1\end{bmatrix}.$$

In other words, a (right) circulant matrix is a matrix obtained by stacking cyclically right-shifted versions of the top row vector. There is a linear isomorphism circ between $\mathbb{R}^n$ and the set of $n\times n$ circulant matrices: given $c\in\mathbb{R}^n$, $\mathrm{circ}(c)$ is the circulant matrix with first row equal to c and with ith row, for $i\in\{2,\dots,n\}$, equal to c right-shifted $(i-1)$ times. For example, the last equation says $C = \mathrm{circ}(c_1,\dots,c_n)$.

The *representer* of an $n\times n$ circulant matrix $C = \mathrm{circ}(c_1,\dots,c_n)$ is the polynomial $p_C(s) = c_1 + c_2s + \cdots + c_ns^{n-1}$. For $\omega_n = \exp(2\pi\sqrt{-1}/n)$, let $F_n\in\mathbb{C}^{n\times n}$ be the *Fourier matrix of order* n given by

$$F_n^* = \frac{1}{\sqrt{n}}\begin{bmatrix}1 & 1 & 1 & \cdots & 1\\ 1 & \omega_n & \omega_n^2 & \cdots & \omega_n^{n-1}\\ 1 & \omega_n^2 & \omega_n^4 & \cdots & \omega_n^{2(n-1)}\\ \vdots & \vdots & \vdots & & \vdots\\ 1 & \omega_n^{n-1} & \omega_n^{2(n-1)} & \cdots & \omega_n^{(n-1)(n-1)}\end{bmatrix}.$$

Theorem A.1 (Diagonalization of circulant matrices): If $C\in\mathbb{R}^{n\times n}$ is circulant, then its eigenvalues are $\lambda_i = p_C(\omega_n^i)$, for $i\in\{1,\dots,n\}$, and

$$C = F_n^*\,\mathrm{diag}(\lambda_1,\dots,\lambda_n)F_n.$$